

Irradiation in CH<sub>3</sub>OD under identical conditions afforded **6** and **7** without detectable (300-MHz <sup>1</sup>H NMR analysis) deuterium incorporation.

**DCN-Sensitized Irradiation of (Z)-2-Methoxy-1,3,3-triphenylpropene (7).** Vinyl ether **7** (9 mg) and DCN (3 mg) in methanol (10 mL) were irradiated through Pyrex with 350-nm lamps for 19 h. Both **6** and **7** are observed (ca. 4:1) by HPLC and <sup>1</sup>H NMR analysis.

**DCN-Sensitized Irradiation of 2-Methoxy-1,1,3-triphenylpropene (8).** Vinyl ether **8** (10 mg) and DCN (3 mg) in methanol (10 mL) were irradiated through Pyrex with 350-nm lamps for 18 h. Analysis by HPLC and <sup>1</sup>H NMR showed only unreacted **8**. No deuterium incorporation was detected in **8** when irradiation was performed in CH<sub>3</sub>OD.

**DCA-Sensitized Irradiation of Triphenylallene in Methanol-d.** Allene **4** (500 mg) and DCA (60 mg) in methanol-*d* (170 mL) at 0 °C were irradiated through a uranium filter for 4 h. The solvent was removed by vacuum distillation at 0 °C and the residue was subjected to flash chromatography (2.0 × 31 cm) with hexane elution in 100-mL fractions: 1-2, nil; 3-9, 353 mg of **4**; 10-11, 2 mg of **5**; elution with 0.1% ether-hexane: 12-25, nil; 26-30, 31 mg of **6**, **7**, and **8**; 31-35, nil; 36-47, 24 mg of **10** and **11**.

Recovered allene **4** was recrystallized from pentane and determined to be 18% deuterated by mass spectroscopic analyses. Propyne **5** was further purified by HPLC; the <sup>1</sup>H NMR spectrum showed no detectable propargylic resonance. Vinyl ethers **6**, **7**, and **8** were separated by preparative TLC. <sup>1</sup>H NMR analysis showed each to be 100% *d*<sub>1</sub> within experimental error, with deuterium exclusively at the allylic positions. Dimers **10** and **11** were undeuterated within limits of detection.

**DCN-Sensitized Irradiation of Triphenylpropyne in Methanol-d.** Propyne **5** (500 mg) and DCN (150 mg) in methanol-*d* (170 mL) at 0 °C were irradiated through a Pyrex filter for 4 h. The solvent was removed by vacuum distillation at 0 °C and the residue was subjected to flash chromatography (2.0 × 31 cm) with hexane elution in 100-mL fractions: 1-5, nil; 6-7, 24 mg of **4**; 8-13, 81 mg of **5**; 14-19, nil; 20-32, 149 mg of **6**; 33-34, nil; 35-50, 46 mg of **7**; elution with 1.0% ether hexane: 51-52, 10 mg of **7** and **8**, ca. 1.0:0.8; 53-54, 78 mg of **8**; elution with 10% ether-hexane: 55-56, 60 mg of DCN adducts; 57-60, 100 mg of DCN.

Deuterium distribution in products from runs at 8, 30, and 84% conversion was determined by integration vs. the methoxy singlet. Results are described in the text.

**Quantitative HPLC Analysis of Sensitized Reactions.** Irradiations were conducted at -10 °C. Aliquots (5 mL) of the reaction solution were removed at intervals during the irradiation and analyzed as follows. Internal standard 1,1-bis(4-methoxyphenyl)ethylene and reaction solution (2 mL) were combined, concentrated in vacuo, and extracted with 20% ether-hexane (1.0 mL). The extract was filtered through a plug of alumina (1.5 cm) and then analyzed by HPLC (0.25% ether-hexane,  $\mu$ -Porasil). Results in Table I (see text) are the average of five determinations. Representative HPLC retention times were as follows: **4** (3.3 min), **5** (3.8 min), **6** (6.5 min), **7** (9.3 min), **8** (11.1 min), **10** (12.5 min), **11** (14.2 min).

**Quantitative DCA-Sensitized Irradiation of Triphenylallene (4).** Allene **4** (200 mg) and DCA (54 mg) in methanol (200 mL) at -10 °C were irradiated with 350-nm lamps for 5 h. At this time, significant quantities of precipitated dimers **10** and **11** were observed.

**Quantitative DCN-Sensitized Irradiation of Triphenylallene (4).** Allene **4** (200 mg) and DCN (100 mg) in methanol at -10 °C were irradiated with the 300-nm lamps for 3 h.

**Quantitative DCN-Sensitized Irradiation of Triphenylpropyne (5).** Propyne **4** (200 mg) and DCN (56 mg) in methanol (200 mL) at -10 °C were irradiated with 300-nm lamps for 4 h.

**Acknowledgment.** We are grateful to the National Science Foundation for support of this research and to Mr. Jim Benson for the X-ray structure of dimer **11**.

**Registry No.** **4**, 966-87-0; **5**, 5467-43-6; **6**, 98540-15-9; **7**, 98540-16-0; **8**, 98540-17-1; **10**, 98540-18-2; **11**, 98540-19-3; **12**, 98540-20-6; **13**, 98540-21-7; DCA, 1217-45-4; DCN, 3029-30-9.

**Supplementary Material Available:** Coordinates and thermal parameters for dimer **11** (4 pages). Ordering information is given on any current masthead page.

## [2.2](1,4)Phenanthrenoparacyclophane: Synthesis and Two-Dimensional Proton and Carbon-13 NMR Study<sup>1</sup>

Henning Hopf,\*<sup>†</sup> Cornelia Mlynek,<sup>†</sup> Sayed El-Tamany,<sup>†</sup> and Ludger Ernst\*<sup>†</sup>

*Contribution from the Institut für Organische Chemie, Technische Universität Braunschweig, Hagenring 30, D-3300 Braunschweig, West Germany, and the Gesellschaft für Biotechnologische Forschung, Mascheroder Weg 1, D-3300 Braunschweig, West Germany.*

*Received February 28, 1985*

**Abstract:** A new method for the preparation of condensed [2.2]paracyclophanes is discussed and realized for the case of [2.2](1,4)phenanthrenoparacyclophane (**7**). This hydrocarbon may be prepared in three steps from [2.2]paracyclophane (**4**) by formylation, Wittig-Horner olefination, and photocyclization of the stilbene intermediate **6**. The 300-MHz <sup>1</sup>H and 75-MHz <sup>13</sup>C NMR spectra of **7** were completely assigned, without the use of chemical shift arguments, by <sup>1</sup>H{<sup>1</sup>H} NOE difference spectroscopy and two-dimensional homo- and heteronuclear chemical shift correlation. Shift correlations via long-range couplings <sup>n</sup>J<sub>HH</sub> and <sup>n</sup>J<sub>CH</sub> were also carried out to assign the bridge proton and quaternary carbon resonances, respectively. The combined ring current effect of the two annelated aromatic rings was estimated with the Johnson-Bovey model and was compared to the experimental results. There exists a qualitative correlation between the estimated and the experimental <sup>1</sup>H chemical shift differences of **7** and **4** but no such correlation for <sup>13</sup>C shifts.

[2.2]Cyclophanes containing one or more condensed aromatic subunits (general structure **3**) have been studied extensively in recent years because of their interesting stereochemical and electronic properties. They have, furthermore, been used as precursors of topologically novel compounds such as the circulenes, propellenes, paddlanes, and helicene-derived cyclophanes, to name but a few.<sup>2</sup> For the synthesis of **3**, the presently most

common approach begins with the preparation of the future aromatic subunits **1** and **2**. Depending on the structural complexity of these building blocks, the synthetic workup to this point may be quite demanding. The second half of the synthesis normally

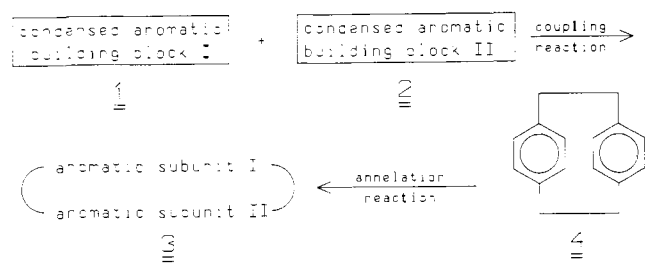
(1) This is part 24 of our cyclophane series. For part 23 see: Hopf, H.; Raulfs, F.-W. *Isr. J. Chem.* **1985**, *25*, 210-216.

(2) For an up-to-date symmetry see Reiss, J. A. In "Cyclophanes"; Keehn, P. M.; Rosenfeld, S. M., Eds.; Academic Press: New York, 1983; Vol. 2, Chapter 7, pp 443-484.

<sup>†</sup> Universität Braunschweig.

<sup>†</sup> Gesellschaft für Biotechnologische Forschung.

## Scheme I



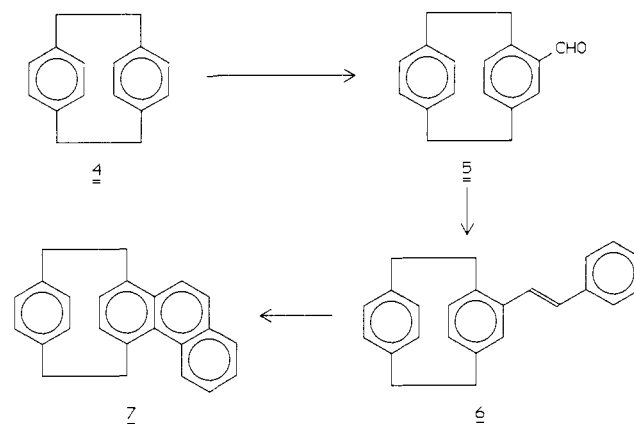
consists of a coupling reaction that generates the [2.2]phane system either directly or via intermediates that are usually converted to the target molecule by ring contraction processes (Scheme I).

The most widely used coupling of the former type proceeds via *p*-xylylenes (commonly generated from the aromatic substrates by 1,6-Hofmann elimination), whereas bis sulfur intermediates are often employed in the latter approach (C–C bond formation by sulfone pyrolysis, S-analogous Stevens rearrangement, or related processes<sup>2,3</sup>). Possibly because of the success of this general strategy, an alternative that may be regarded as the reverse of the above approach (1 + 2 → 3) has been neglected: rather than *ending*, this route *begins* with a phane system, for example with [2.2]paracyclophane (4) itself, which may be regarded as the parent system of the condensed benzenoid paracyclophanes 3. To generate these hydrocarbons all that is required is to subject derivatives of 4 to any of the numerous known annelation processes. In fact, [2.2](1,4)naphthalenoparacyclophane was prepared by Cram and co-workers from 4 by succinylation, ring closure, reduction, and aromatization in 1963.<sup>4</sup> Because of its many steps, relatively low overall yield, and the (formerly) high price of 4 this methodology has found only limited applications.

However, 4 is now a readily available starting material supplied by all major producers of fine chemicals, and other condensation reactions that are both preparatively simpler and of greater structural variability should be considered.<sup>5</sup> We are particularly interested in applying the stilbene-phenanthrene photocyclization to the synthesis of condensed [2.2]paracyclophanes. Although this photoreaction has been employed previously for the preparation of bridged aromatic molecules,<sup>2,6a-k</sup> we are only aware of a single example<sup>7</sup> in which the benzene ring of a [2.2]paracyclophane participates in this widely used organic photoreaction.<sup>8a,b</sup>

The present paper describes the synthesis of [2.2](1,4)-phenanthrenoparacyclophane (7) from 4 in three preparatively simple steps. Furthermore, it seemed desirable to determine the structure of 7 by a combined analysis of its proton and <sup>13</sup>C NMR

## Scheme II



spectra, applying a variety of the recently developed one- and two-dimensional techniques. Although the chemical shifts and coupling constants of the aromatic protons of numerous cyclophanes have been reported and discussed, knowledge of the NMR parameters of the molecular bridge protons of these molecules is scarce. In fact, we know of no complex [2.2]paracyclophane for which the coupling pattern of the ethano bridges has been completely analyzed.<sup>9</sup>

**Synthesis (Scheme II).** For the preparation of 7 [2.2]paracyclophane (4) is first formylated by the Rieche reaction<sup>10</sup> as described previously<sup>1,11</sup> (yield 93%). Chain elongation of 5 by the Wittig-Horner reaction with diethyl benzylphosphonate provides 4-styryl[2.2]paracyclophane 6 (a "stilbenophane") in 59% yield. The *trans* configuration of the double bond is established by a coupling constant of 16.0 Hz for the olefinic protons. Irradiation of the colorless solid 6 in cyclohexane in the presence of iodine and air with a mercury high-pressure lamp for 3 h at room temperature followed by preparative thick-layer chromatography on silica and recrystallization (ethanol) provides analytically pure 7 in 31% yield. The structure proof of this novel phenanthrenophane rests on the usual analytical and spectroscopic data (see Experimental Section), especially on its high-field NMR spectra discussed in the following section. Since derivatives of both the paracyclophane moiety and the phosphonate are available<sup>12</sup> or may be readily prepared by routine methods, we consider the above sequence to be of general value for the preparation of condensed [2.2]paracyclophanes.

## NMR Investigation of 7

The structure of [2.2](1,4)phenanthrenoparacyclophane is proved unambiguously by the results of the combined analyses of its <sup>1</sup>H and <sup>13</sup>C NMR spectra, which are described below. In order to study the influence of the particular geometry of this compound on both <sup>1</sup>H and <sup>13</sup>C chemical shifts, we carried out a complete assignment of both types of spectra. To avoid circular reasoning in the discussion, no chemical shift arguments are put forward for any assignment. Instead we applied a variety of recently developed one- and two-dimensional techniques, the results of which allow clear-cut assignments without the need of auxiliary argumentation. Apart from an iterative analysis of the <sup>1</sup>H NMR spectrum, the following techniques were employed: standard two-dimensional (2D) <sup>1</sup>H/<sup>1</sup>H chemical shift correlation spectroscopy (COSY)<sup>13</sup> and the corresponding version of this ex-

(3) For comprehensive reviews see: Vögtle, F.; Neumann, P. *Synthesis* **1973**, 85–103. Mitchell, R. H. *Heterocycles* **1978**, *11*, 563.

(4) Cram, D. J.; Dalton, C. K.; Knox, G. R. *J. Am. Chem. Soc.* **1963**, *85*, 1088–1093.

(5) For the synthesis of [2.2](1,4)naphthalenoparacyclophane from 4,5,12,13-tetrakis(methoxycarbonyl)[2.2]paracyclophane by double annelation see: Hopf, H.; Kleinschroth, J. *Tetrahedron Lett.* **1978**, 969–972. cf. Hopf, H.; Kleinschroth, J.; Böhm, I. *Org. Synth.* **1981**, *60*, 41–48.

(6) (a) Lawson, J.; DuVernet, R.; Boekelheide, V. *J. Am. Chem. Soc.* **1973**, *95*, 956–957. (b) Potter, S. E.; Sutherland, I. O. *J. Chem. Soc., Chem. Commun.* **1973**, 520–521. (c) DuVernet, R. B.; Otsubo, T.; Lawson, J. A.; Boekelheide, V. *J. Am. Chem. Soc.* **1975**, *97*, 1629–1630. (d) Jessup, P. J.; Reiss, J. A. *Tetrahedron Lett.* **1975**, 1453–1456. cf. Jessup, P. J.; Reiss, J. A. *Aust. J. Chem.* **1976**, *29*, 173–178. (e) Thulin, B.; Wennerström, O. *Acta Chem. Scand., Ser. B* **1976**, *B30*, 688–690. (f) Jessup, P. J.; Reiss, J. A. *Aust. J. Chem.* **1976**, *29*, 1267–1275. (g) Mitchell, R. H.; Carruthers, R. J.; Mazuch, L. *J. Am. Chem. Soc.* **1978**, *100*, 1007–1008. (h) Otsubo, T.; Gray, R.; Boekelheide, V. *J. Am. Chem. Soc.* **1978**, *100*, 2449–2456. (i) Diederich, F.; Staab, H. A. *Angew. Chem., Int. Ed. Engl.* **1978**, *17*, 372. cf. Krieger, C.; Diederich, F.; Schweitzer, D.; Staab, H. A. *Angew. Chem., Int. Ed. Engl.* **1979**, *18*, 699. (j) Thulin, B.; Wennerström, O. *Acta Chem. Scand., Ser. B* **1983**, *B37*, 297–301. (k) Thulin, B.; Wennerström, O. *Acta Chem. Scand., Ser. B* **1983**, *B37*, 589–595.

(7) Tribout, J.; Martin, R. H.; Doyle, M.; Wynberg, H. *Tetrahedron Lett.* **1972**, 2839–2842.

(8) For two very recent reviews see: (a) Laarhoven, W. H. *Recl. Trav. Chim. Pays-Bas* **1983**, *102*, 185–204 and 241–254. (b) Mallory, F. B.; Mallory, C. W. *Org. React. (N.Y.)* **1984**, *30*, 1–456.

(9) Mitchell, R. H. In "Cyclophanes"; Keehn, P. M., Rosenfeld, S. M. Eds.; Academic Press: New York, 1983; Vol. 1, Chapter 4, pp 239–310.

(10) Rieche, A.; Gross, H.; Höft, E. *Chem. Ber.* **1960**, *93*, 88–94.

(11) (a) Hopf, H.; Eltamany, S. *Chem. Ber.* **1983**, *116*, 1682–1685. (b) Hopf, H.; Eltamany, S.; Raulfs, F. W. *Angew. Chem., Int. Ed. Engl.* **1983**, *22*, 633.

(12) We have previously described the synthesis of all possible dialdehydes with one formyl group per benzene ring; cf. ref. 1 and Broschinski, K. Ph.D. Dissertation, Universität Braunschweig, Braunschweig, West Germany, 1984.

(13) (a) Bax, A.; Freeman, R.; Morris, G. J. *Magn. Reson.* **1981**, *42*, 164–168. (b) Bax, A.; Freeman, R. *J. Magn. Reson.* **1981**, *44*, 542–561.

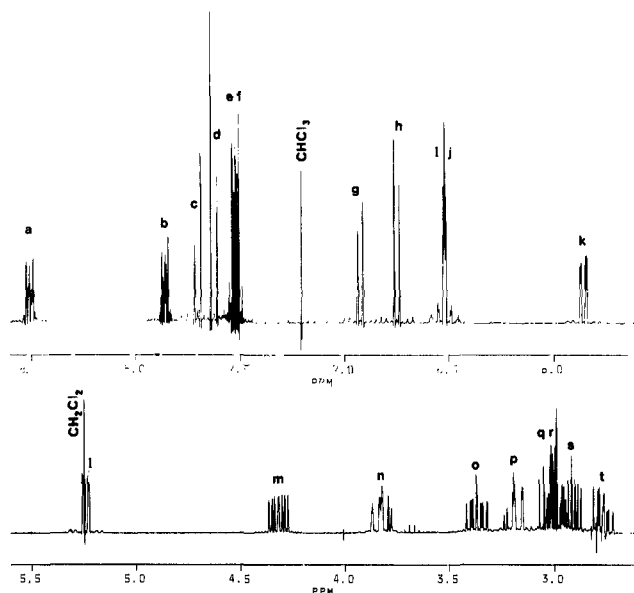


**Figure 1.** 300-MHz  $^1\text{H}$  NMR spectrum of **7** in  $\text{CDCl}_3$ . Proton signals are labeled a-t from high to low frequency. Spinning sidebands were caused by a broken insert in the probe head.

**Table I.**  $^1\text{H}$  NMR Data for **7** in  $\text{CDCl}_3$  Solution<sup>a</sup>

proton	$\delta$	proton	$\delta$
a	8.511	k	5.856
b	7.864	l	5.242
c	7.703	m	4.318
d	7.629	n	3.827
e	7.529	o	3.369
f	7.520	p	3.187
g	6.926	q	3.020
h	6.752	r	2.984
i	6.532	s	2.912
j	6.511	t	2.768
protons	$J$ , Hz	protons	$J$ , Hz
ab	0.6	kl	7.8
ac	0.7	mo	-14.5
ae	8.5	ms	4.7
af	1.2	mt	8.5
am	0.6 <sup>b</sup>	np	1.6
be	1.4	nq	-13.7
bf	8.0	nr	10.0
cd	8.9	os	8.8
ef	6.9	ot	6.3
gh	7.5	pq	10.4
go	0.9 <sup>b</sup>	pr	-13.2
ij	7.9	qr	7.1
ik + il	1.8	st	-13.4
jk + jl	1.8		

<sup>a</sup> Measured at 300 MHz relative to internal  $\text{Me}_4\text{Si}$ , chemical shifts  $\pm 0.001$  ppm, coupling constants  $\pm 0.1$  Hz. <sup>b</sup> Sign unknown.

periment that emphasizes long-range coupling constants (COSY-LR);<sup>13b,14</sup> heteronuclear  $^{13}\text{C}/^1\text{H}$  2D shift correlation experiments,<sup>15</sup> also using both large ( $J_{\text{CH}}$ ) and small<sup>14</sup> (long-range, i.e.  $^nJ_{\text{CH}}$ ) C,H couplings; and  $^1\text{H}\{^1\text{H}\}$  nuclear Overhauser enhancement (NOE) difference spectroscopy.<sup>16</sup> A few homonuclear decoupling experiments served to verify some unexpected long-range H,H coupling constants.

To facilitate the description of the analysis, the protons of **7** are labeled with lower case letters a to t, in the order in which their resonances appear from high to low frequency, and the carbon

(14) Hull, W. E. "Two-Dimensional NMR"; Bruker Analytische Messtechnik: Karlsruhe, 1982.

(15) (a) Maudsley, A. A.; Müller, L.; Ernst, R. R. *J. Magn. Reson.* **1977**, *28*, 463-469. (b) Bodenhausen, G.; Freeman, R. *J. Magn. Reson.* **1977**, *28*, 471-476. (c) Bax, A.; Morris, G. A. *J. Magn. Reson.* **1981**, *42*, 501-505.

(16) Sanders, J. K. M.; Merz, J. D. *Prog. Nucl. Magn. Reson. Spectrosc.* **1982**, *15*, 353-400, in particular 361-380.

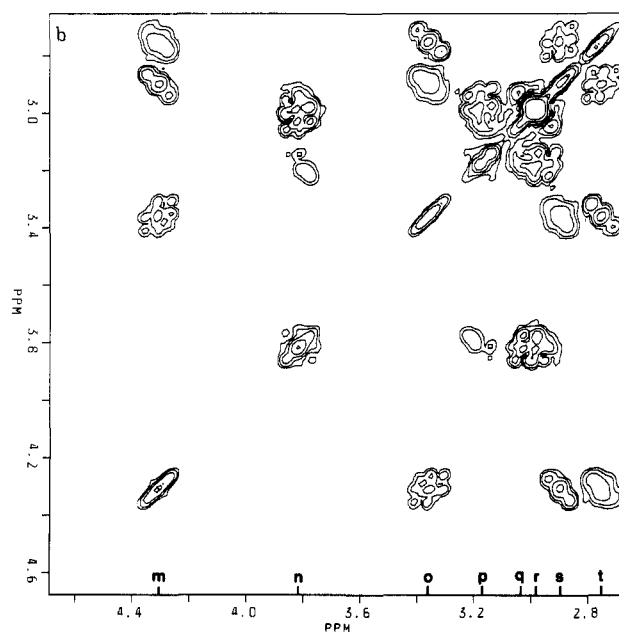
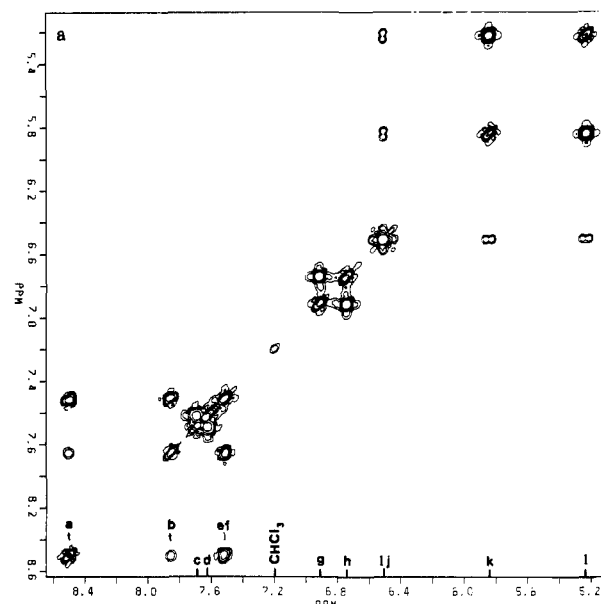


**Figure 2.** 300-MHz  $^1\text{H}/^1\text{H}$  chemical shift correlation map (COSY-45) of **7**: (a) aromatic protons; (b) methylene protons.

**Table II.** Results of 2D Homonuclear Correlation Spectra (COSY)

spin system	protons involved <sup>a</sup>	spin system	protons involved <sup>a</sup>
1	a, b, e, f	4	i, j, k, l
2	c, d	5	m, o, s, t
3	g, h	6	n, p, q, r
long-range couplings detected <sup>b</sup>	cross peak intensities	long-range couplings detected <sup>b</sup>	cross peak intensities
ab, ac, am		ip, ir	ip > ir
bc		js, jt	js > jt
dn		kp, kr	kr > kp
gm, go	go > gm	ls, lt	lt > ls
hn, hq	hq > hn		

<sup>a</sup> Neglecting inter-ring and benzylic couplings. <sup>b</sup> In "long-range version" of the COSY experiment.

atoms are labeled correspondingly with capital letters A to X.

The 300-MHz proton NMR spectrum of [2.2](1,4)-phenanthrenoparacyclophane is depicted in Figure 1, which shows well-separated resonances apart from those for the pairs of protons e/f, i/j, and q/r. The chemical shifts and H,H coupling constants that follow from the iterative analyses are given in Table I. Before

**Table III.**  $^1\text{H}\{^1\text{H}\}$  Nuclear Overhauser Enhancements in **7**

proton resonance irradiated	proton resonances enhanced	proton resonance irradiated	proton resonances enhanced
a	e/f(10%), m(17%)	g	o(8%), i/j(4%)
b	c(6%), e/f(6%)	h	q(7%), i/j(3%)
c <sup>a</sup>	b(4%), [n(4%)]	k	l(11%), r(7%)
d	k(4%), n(12%)	l	k(10%), t(5%)

<sup>a</sup> Proton d also affected due to lack of selectivity.

these calculations could be carried out, it was necessary to determine which protons formed common spin systems, neglecting long-range couplings. This was achieved by a 2D  $^1\text{H}/^1\text{H}$  chemical shift correlation spectrum. The COSY-45 version<sup>13b</sup> of the experiment was used because it not only streamlines the diagonal in the correlation map, thus facilitating recognition of cross peaks that lie close to it, but it also permits, in favorable cases, the determination of the relative signs of coupling constants, thus aiding the assignment.

The aromatic region of the COSY spectrum (Figure 2a, Table II) shows two four-proton spin systems, viz., (a, b, e, f) and (i, j, k, l) and two two-proton systems, viz., (c, d) and (g, h). The one-dimensional spectra of these systems were then treated by iterative analysis. The coupling constants  $J_{\text{HH}}$  (Table I) show that the system (a, b, e, f) is due to the outer unsubstituted phenanthrene ring, (i, j, k, l) to the para-disubstituted benzene ring, (c, d) to the middle phenanthrene ring because of its large 8.9-Hz ortho coupling, and (g, h) to the outer disubstituted phenanthrene ring. According to the aliphatic part of the COSY spectrum (Figure 2b), protons m, o, s, and t belong to one  $\text{CH}_2\text{CH}_2$  bridge and protons n, p, q, and r to the other one. Each of the bridge protons is involved in one geminal and in two vicinal spin-spin couplings. Considering the cross peaks of m with o, s, and t, it is evident that the (positive) slope of the m/o cross peak is opposed to the slopes of the m/s and m/t cross peaks. This demonstrates<sup>13b</sup> that the sign of  $J_{\text{mo}}$  is opposite to the signs of  $J_{\text{ms}}$  and  $J_{\text{mt}}$ ; i.e.,  $J_{\text{mo}}$  is the geminal coupling constant. In other words, protons m and o are connected to the same carbon atom and, by default, s and t to the adjacent one (also visible from the slope of their cross peak). The situation is not quite so clear for the second bridge spin system because of the overlap of the n/q and n/r cross peaks. However, the n/p cross peak with its negative slope indicates a vicinal coupling between these protons, in analogy to m/s and m/t, and the overlapping n/q and n/r cross-peak pattern is better interpreted by n/q having a positive and n/r a negative slope than vice versa. This would suggest protons n and q being bonded to the same carbon. This interpretation is confirmed later by the  $^{13}\text{C}/^1\text{H}$  shift correlation. The results of the COSY experiment greatly facilitated the iterative analyses of the bridge-proton 1D spectra.

As pointed out above, the chemical shifts obtained from the spectral analysis were deliberately not used to achieve an assignment of the spectrum. Therefore, other techniques had to be applied to determine the relative spatial location of protons belonging to different spin systems. A series of homonuclear NOE difference spectra<sup>16</sup> was therefore taken (Table III).

Irradiation of the a multiplet caused a strong enhancement (17%) of the m resonance (Figure 3, middle trace) and allowed the latter to be assigned to the methylene proton, which is close in space to the single phenanthrene "bay proton". Together with the result of the iterative analysis this determines the location of protons a, b, e, f, m, and o. Irradiation of the b resonance enhanced the doublet of proton c, and a strong intensity increase (12%) of d was observed upon irradiation of the n multiplet (Figure 3, top trace). This allowed us to locate protons c, d, n, and q. NOEs between g and o and between h and q demonstrated the ortho relations of the two remaining phenanthrene protons and the benzylic protons in question. The relative orientation of the protons of the para-disubstituted benzene ring and the phenanthrene protons resulted from the observation of a moderate NOE between d and k. Irradiation of protons k and l showed enhancements of the r and t multiplets, respectively, thus completing the assignment

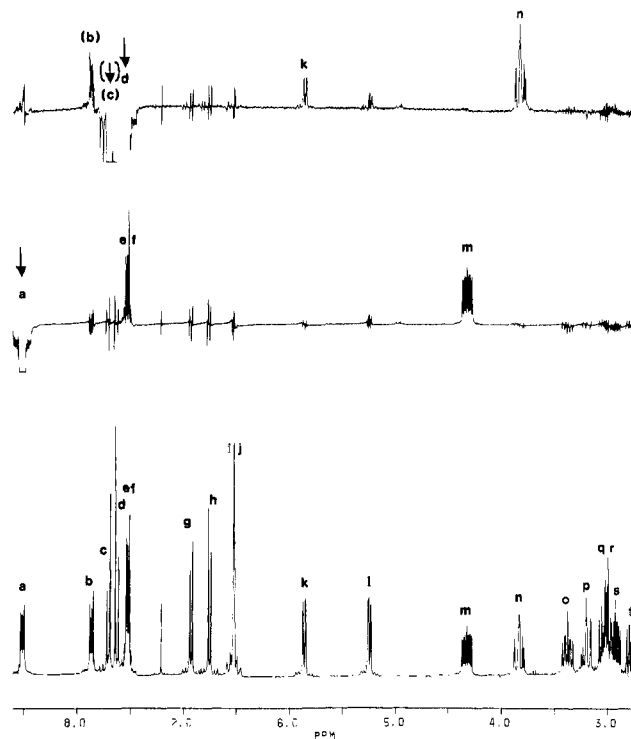


**Figure 3.** NOE difference spectra of **7**: irradiation of  $\text{H}_d$  (top) and of  $\text{H}_a$  (middle) and control spectrum (bottom).

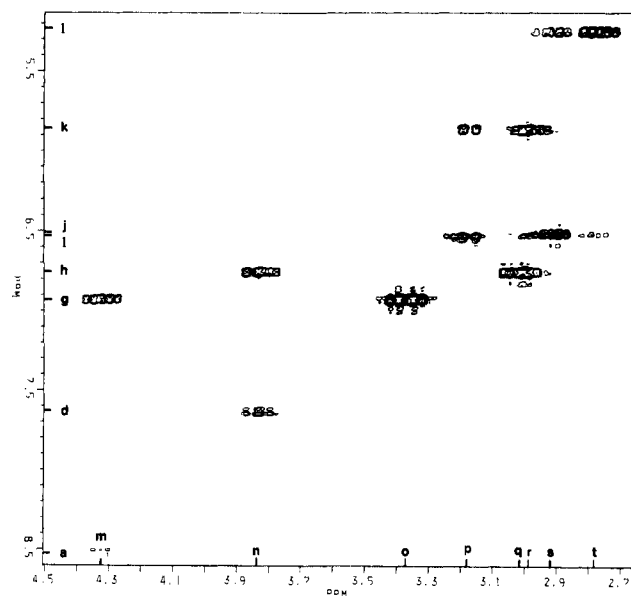


**Figure 4.** Cross-peaks in the  $^1\text{H}/^1\text{H}$  chemical shift correlation map of **7** obtained in the "long-range" version of the experiment.

of the chemical shifts to all 20 protons in the molecule.

Many of the results of the NOE experiments were confirmed by a second  $^1\text{H}/^1\text{H}$  chemical shift correlation experiment that was optimized for long-range coupling constants (COSY-LR) by inserting an extra delay<sup>13b,14</sup> after each of the two pulses. The shift correlation map contained cross peaks (Figure 4) for all ortho-benzylic couplings. These were not resolved in the 1D spectrum. Interestingly, the cross peaks representing couplings between aromatic and syn-benzylic protons (e.g.,  $J_{\text{hq}}$ ) always had distinctly higher intensities than cross peaks for couplings to anti-benzylic protons (e.g.,  $J_{\text{hn}}$ ); see Table II. The cross peak intensities, however, do not necessarily correlate with the sizes of the coupling constants.<sup>13b</sup> The COSY-LR experiment also showed the presence of long-range couplings,  $J_{\text{ab}}$ ,  $J_{\text{ac}}$ , and  $J_{\text{bc}}$  as expected. Surprisingly, however, correlations were also found between protons a and m and between d and n. Since these pairs of protons are at a distance

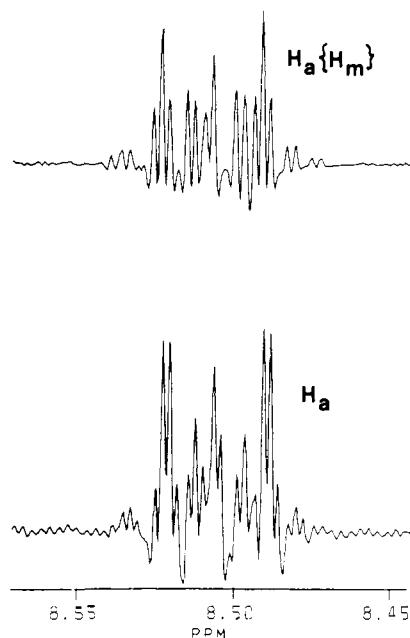


**Figure 5.**  $^1\text{H}$  NMR absorption of proton  $\text{H}_a$  in **7**: normal spectrum (bottom), with simultaneous decoupling of  $\text{H}_m$  (top).

of six and five bonds from each other, respectively, and since the intervening bonds are not arranged in a fashion that would particularly favor spin-spin coupling, the interactions  $J_{am}$  and  $J_{dn}$  can be considered to be cases of relatively rare  $^1\text{H}/^1\text{H}$  through-space couplings.<sup>17</sup> As opposed to  $J_{dn}$ , the coupling  $J_{am} = 0.6$  Hz is resolved in the 1D spectrum. It is verified by the change of the pattern of multiplet a when proton m is decoupled (Figure 5).

The assignment of the  $^{13}\text{C}$  NMR spectrum of **7** would not be possible by conventional methods. Selective decoupling would fail because of several near-degenerate  $^1\text{H}$  chemical shifts in the aromatic region and because of the complexity of the methylene proton absorptions. Investigation of the  $^{13}\text{C},^1\text{H}$  coupling pattern in a proton-coupled spectrum allowed the assignments of only the  $^{13}\text{C}$  resonances T and Q. The former shows no vicinal  $J_{\text{CH}}$  couplings and the latter displays only one vicinal coupling of 5.5 Hz, which is indicative<sup>18</sup> of a cisoid arrangement of the coupled nuclei. For the remaining resonances of the proton-bearing carbon atoms the splitting pattern was either not characteristic or it was not recognizable because of signal overlap. The multiplicities of the quaternary carbon resonances could not be determined due to sensitivity reasons. A viable alternative consisted of recording 2D  $^{13}\text{C}/^1\text{H}$  chemical shift correlation spectra. Two separate experiments were carried out. In the first one, the recent pulse sequence by Rutar<sup>19</sup> was applied, which suppresses vicinal and longer range  $^1\text{H},^1\text{H}$  coupling constants in the  $F_1$  dimension, thereby increasing the sensitivity of the experiment and permitting the application of the technique to smaller amounts of sample.<sup>20</sup> The aromatic region of the shift correlation matrix (Figure 6a) shows singlet cross peaks at the chemical shifts of the proton-bearing carbons and allows straightforward assignment of all the respective  $^{13}\text{C}$  resonances.

Rutar's pulse sequence does not suppress couplings between protons that are bonded to the same  $^{13}\text{C}$  nucleus, so the geminal  $J_{\text{HH}}$  appear in the  $F_1$  traces whenever methylene protons are

(17) (a) Review: Hilton, J.; Sutcliffe, L. H. *Prog. Nucl. Magn. Reson. Spectrosc.* **1975**, *10*, 27-39. (b) recent examples: de Kowalewski, D. G.; Contreras, R. H.; Engelmann, A. R.; Facelli, J. C.; Durán, J. C. *Org. Magn. Reson.* **1981**, *17*, 199-203. Schaefer, T.; Laatikainen, R. *Can. J. Chem.* **1983**, *61*, 224-229.

(18) Ernst, L. *Chem. Ber.* **1975**, *108*, 2030-2039.

(19) (a) Rutar, V. *J. Magn. Reson.* **1984**, *58*, 306-310. (b) Wong, T. C.; Rutar, V. *J. Am. Chem. Soc.* **1984**, *106*, 7380-7384. cf. also Bax, A. *J. Magn. Reson.* **1983**, *53*, 517-520.

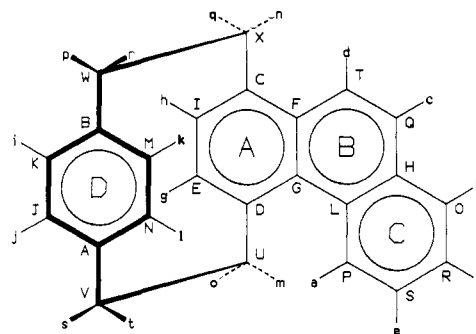
(20) For another application see: Ernst, L. *J. Chem. Soc., Perkin Trans. 1* **1984**, 2267-2270.

**Table IV.**  $^{13}\text{C}$  NMR Data of **7** in  $\text{CDCl}_3$  Solution<sup>a</sup>

carbon	$\delta$	$m^b$	proton(s) involved in		$J_{\text{CH}},^d$ Hz
			$^1J_{\text{CH}}^c$	$^nJ_{\text{CH}}^c$	
A	138.77	s		i + k	$^1J = 157.6, ^3J = 7.1$ and 5.2
B	137.93	s		(j + l), <sup>e</sup> p	
C	136.83	s		g + n	
D	136.39	s		h + m + o + s	
E	134.26	d	g		
F	134.13	s		c + h + q	
G	132.97	s		d + g + o	
H	132.32	s		d	
I	131.98	d	h		
J	131.95	d	j		f
K	131.70	d	i		g
L	130.90	s		c + e	$^1J \approx 158, ^3J \approx 6^h$
M	129.11	d	k		
N	128.46	d	l		g
O	128.22	d	b		f
P	128.10	d	a		f
Q	126.04	d	c		$^1J = 160.1, ^3J = 5.5$
R	125.75	d	f		$^1J = 159.3, ^3J = 8.4$
S	125.48	d	e		$^1J = 158.7, ^3J = 8.7$
T	123.97	d	d		$^1J = 158.0$
U	38.56	t	m + o		g
V	34.82	t	s + t		g
W	34.57	t	p + r		g
X	33.56	t	n + q		g

<sup>a</sup> Measured at 75.5 MHz relative to  $\text{CDCl}_3$ ,  $\delta$  77.05. <sup>b</sup> Multiplicity in single-frequency off-resonance  $^1\text{H}$ -decoupled spectrum. <sup>c</sup> From 2D  $^{13}\text{C}/^1\text{H}$  correlation spectra. <sup>d</sup>  $\pm 0.2$  Hz. <sup>e</sup>  $^nJ_{\text{CH}}$  correlation only visible in the cross-section through the correlation matrix, not in the contour plot (Figure 7). <sup>f</sup> Not determined because of signal overlap. <sup>g</sup> Complex resonance. <sup>h</sup> Average value, quartet multiplicity.

**Chart I**



chemically nonequivalent. In addition, "artifact" peaks appear at the mean  $^1\text{H}$  chemical shift of these methylene protons. The aliphatic part of the shift correlation map (Figure 6b) allows not only the assignment of the methylene carbon signals but it also shows which protons form methylene pairs. The latter information agrees fully with the conclusions derived from the homonuclear shift correlation experiment (see above).

A second  $^{13}\text{C}/^1\text{H}$  shift correlation experiment was carried out to assign the quaternary carbon resonances. The standard pulse sequence was employed with delays optimized for  $^{13}\text{C},^1\text{H}$  coupling constants of 6 Hz. This experiment is usually considered to be quite insensitive because of the loss of magnetization by  $T_2$  relaxation during the relatively long delays involved. However, an overnight run on the 40-mg sample, followed by appropriate data treatment (power spectrum display), gave a completely satisfactory result (Figure 7).

In principle the quaternary carbon atoms should display between three and six long-range C,H couplings which fall into three categories, viz., geminal couplings to aliphatic protons, vicinal couplings to aliphatic protons, and vicinal couplings to aromatic protons. Vicinal couplings to carbons C, F, and G can be of the cisoid and transoid types. Geminal couplings to aromatic protons are small enough (ca. 1 Hz) so that no corresponding cross peaks are expected. Out of the total of 38 long-range C,H couplings,

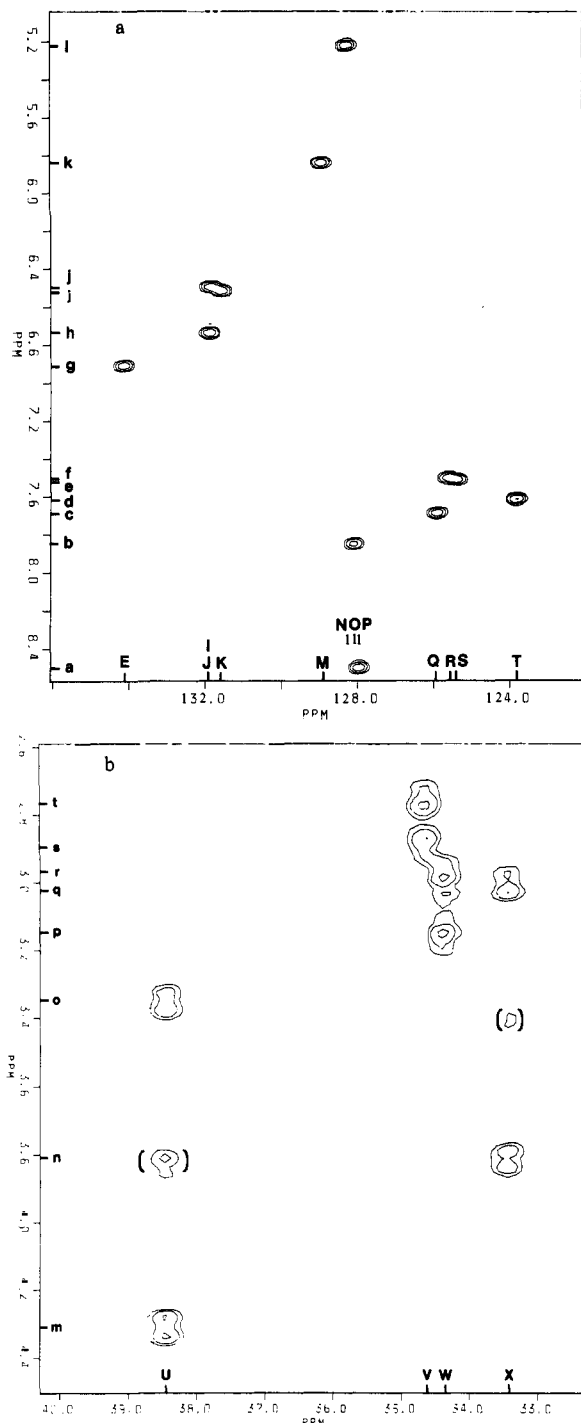


**Figure 6.** 75-MHz/300-MHz  $^{13}\text{C}/^1\text{H}$  chemical shift correlation map of 7: (a) aromatic region; (b) methylene region. Cross peaks in parentheses are due to second-order "artifacts".

18 could be seen as cross peaks in the shift correlation map (Figure 7) and (at least) two more in cross-sections through the correlation matrix (Table IV). This was more than adequate to safely assign all quaternary carbon resonances. Among the cross peaks detected for vicinal C,H interactions, none was due to cisoid coupling. This experiment completes the assignment of the  $^1\text{H}$  and  $^{13}\text{C}$  NMR spectra, which consist of 20 and 24 nonequivalent resonances, respectively. The labels of the chemical shifts in Tables I and IV correspond to the labels of the hydrogen and carbon atoms in Chart I.

## Discussion

The apparently rigid nature of the molecular framework of 7 would seem to keep the two aromatic systems in a relatively fixed

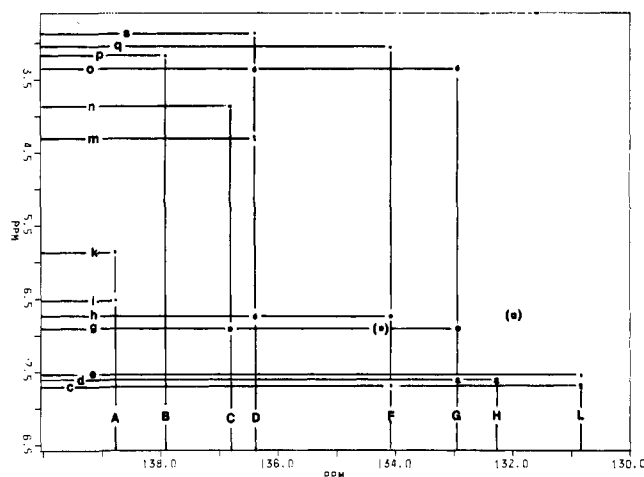


**Figure 7.** Assignment of the quaternary carbon resonances by chemical shift correlation via two- and three-bond C,H coupling. The two cross peaks in parentheses correspond to residual correlations via one-bond couplings.

orientation with respect to one other and to the rest of the molecule. It was therefore tested whether correlations existed between the observed  $^1\text{H}$  or  $^{13}\text{C}$  chemical shifts and calculated ring current shielding effects. Since the exact geometry of the title compound is not known and as it would be inappropriate to describe its geometry by standard bond lengths and angles, the following procedure was adopted. The atomic coordinates of the two aromatic rings A and D that lie over each other and the coordinates of the two bridges connecting them were taken to be those of [2.2]paracyclophane (4), whose structure is known from X-ray diffraction measurements.<sup>21</sup> The two additional benzene rings B and C of the phenanthrene moiety were added on by using bond angles of  $120^\circ$  and bond lengths of 140 and 108 pm for C–C and C–H bonds, respectively. The coordinates of the carbon and hydrogen atoms forming ring D and the methylene bridges and the coordinates of hydrogen atoms g and h on ring A were then calculated relative to the centers of both ring B and ring C and expressed as vertical and lateral displacements in units of benzene ring radii.

Using these displacements, theoretical ring current shifts,  $\delta_B'$ , by ring B, and  $\delta_C'$ , by ring C, were estimated by interpolation or extrapolation of the values given in the tabulation by Johnson and Bovey.<sup>22</sup> The sums of  $\delta_B'$  and  $\delta_C'$ , i.e., the ring current effects caused by the annellation of rings B and C to [2.2]paracyclophane, were then correlated with the differences in chemical shifts between 7 and 4.<sup>23</sup>

**Proton Chemical Shifts.** In Figure 8 the experimental  $^1\text{H}$  shift differences are plotted vs. the Johnson–Bovey ring current shifts  $\delta_B' + \delta_C'$ . The points follow the ideal line with slope 1 and intercept 0 only very roughly, although the data show the proper trend. The most significant deviations from the ideal line are observed for protons k and l. Several possibilities have to be considered to explain the nonideal behavior: (a) Additivity of the effects of rings B and C is not a good assumption. (b) The annellation of standard geometry rings B and C to a [2.2]paracyclophane does not furnish good coordinates for the atoms of these rings. (c) The molecule is not as rigid as assumed in deriving the geometry; e.g., there could be a translation of ring D along the long axis of the naphthalenoid system of rings A and B. This would remove unfa-

(21) (a) Lonsdale, K.; Milledge, H. J.; Rao, K. V. K. *Proc. R. Soc. London, A* **1960**, *255*, 82. (b) Hope, H.; Bernstein, J.; Trueblood, K. N. *Acta Crystallogr. Sect. B: Struct. Crystallogr. Cryst. Chem.* **1972**, *B28*, 1733–1743. The data were obtained from the Cambridge Crystallographic Database.

(22) Bovey, F. A. "Nuclear Magnetic Resonance Spectroscopy"; Academic Press: New York, 1969; Appendix C, pp 264–274.

(23) Chemical shifts for [2.2]paracyclophane in  $\text{CDCl}_3$ : (a)  $^1\text{H}$  (relative to  $\text{Me}_4\text{Si}$ )  $\delta$  3.072 ( $\text{CH}_2$ ) and 6.475 (CH); (b)  $^{13}\text{C}$  (relative to  $\text{CDCl}_3$ ,  $\delta$  77.05)  $\delta$  35.74 ( $\text{CH}_2$ ), 133.06 (CH), and 139.64 (C).

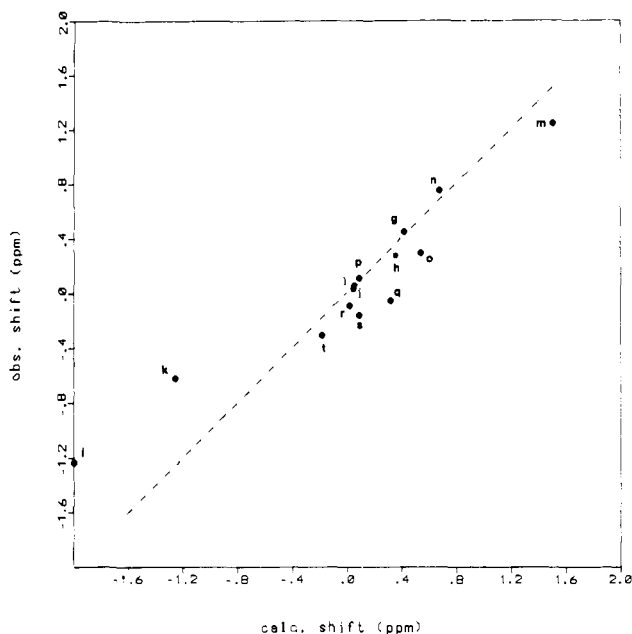


**Figure 8.** Correlation of calculated ring current effects by rings B and C on  $^1\text{H}$  chemical shifts in **7** with observed shift differences between **7** and **4**.

vorable eclipsing interactions between rings A and D. Such translation is observed in the case of *anti*-[2.2](1,4)-naphthalenophane.<sup>24</sup> (d) There are substantial effects other than ring current ones that determine the chemical shifts of the protons under consideration. While none of these possibilities can be excluded altogether, the latter two are likely to be the more important ones. A discussion of item c is postponed until the termination of an X-ray diffraction study, which is planned in our laboratories. A strong hint for the validity of item d is given by the observation that ring substituents in [2.2]paracyclophane cause distinct deshielding of pseudogeminal protons; e.g., in 4-methyl[2.2]paracyclophane (i.e., the mono-*ar*-methyl derivative) the proton of the unsubstituted ring that is situated over the methyl group is deshielded by 0.31 ppm relative to the parent compound.<sup>25</sup> If a correction term of this order is applied to the calculated ring current shifts of points k and l in Figure 8, the discrepancy between experimental and calculated shieldings for these two protons is substantially diminished, yet not removed. On the other hand, a similar deshielding correction would have to be taken into account in the calculated shift of proton m because of the van der Waals interaction<sup>26</sup> with the adjacent proton a. However, this would lead to a larger difference between the experimental and the calculated shift of  $\text{H}_m$ .

**Carbon Chemical Shifts.** As opposed to the situation just discussed for the proton chemical shifts, no useful correlation whatsoever was found between  $^{13}\text{C}$  chemical shifts of [2.2](1,4)phenanthrenoparacyclophane relative to [2.2]paracyclophane<sup>23</sup> and calculated ring current effects of rings B and C. In fact, the experimental  $^{13}\text{C}$  shift differences are generally several times larger than the predicted values of  $\delta_B' + \delta_C'$  and, in some cases, are even of the wrong sign. This indicates that other factors completely outweigh ring current effects on these  $^{13}\text{C}$  shieldings. The chemical shifts affected most by the annellation of rings B and C to [2.2]paracyclophane are those of carbon atoms M, N, U, and X, which differ by  $\Delta\delta$   $-3.95$ ,  $-4.60$ ,  $+2.82$  and  $-2.18$ , respectively, from the shifts of the parent compound. The upfield shifts of atoms M and N are reminiscent of those<sup>25</sup> caused by *ar*-methyl groups on pseudogeminal carbons in [2.2]para-

cyclophanes (e.g.,  $\Delta\delta$   $-5.4$  in the 4-methyl derivative), while the upfield shift of carbon X agrees well with the change of the methyl carbon shift in going from toluene ( $\delta$  21.4) to 1-methylphenanthrene<sup>27</sup> ( $\delta$  19.7). These shifts are essentially due to steric effects as is the shift of carbon U although the latter is downfield. It has its equivalent in the deshielding of the methyl carbon in going from toluene to 4-methylphenanthrene<sup>28</sup> ( $\delta$  27.2, i.e.,  $\Delta\delta$   $= +5.8$ ). The boat shape of ring A causes the steric interaction of the methylene group (carbon U and protons m and o) with the  $\text{C}_p\text{-H}_a$  bond to be substantially smaller than the corresponding interaction of the methyl group with the  $\text{C}^5\text{-H}^5$  bond in 4-methylphenanthrene. This is the reason for the diminished downfield shift of carbon U ( $\Delta\delta$   $= +2.18$ ), for the relative orientation of the interacting groups is known to be an extremely critical factor governing steric shifts.

To summarize the discussion of the chemical shifts, it can be stated that, while there is no quantitative agreement between calculated ring current effects and experimental proton shifts in **7**, there exists a qualitative correlation between these parameters. On the other hand, the  $^{13}\text{C}$  shieldings are mainly governed by factors other than ring current effects.

**Proton-Proton Coupling Constants.** According to a recent review,<sup>9</sup> there are no detailed analyses available of  $^1\text{H}$  NMR spectra of the methylene bridges in substituted [2.2]paracyclophanes. In the present work, the spectra of both bridges of **7** (in which all protons are nonequivalent) have been completely analyzed so that all geminal and vicinal  $^1\text{H}$ ,  $^1\text{H}$  coupling constants are available.

The geminal H,H coupling in [2.2]paracyclophane is not known, but from the study of a series of mono- and di-*ar*-substituted derivatives,<sup>25</sup> we estimate it to lie between  $-12.9$  and  $-13.4$  Hz. Of the four  $^2J_{\text{HH}}$  values in [2.2](1,4)phenanthrenoparacyclophane (Table I), two fall into this range, viz., those of the methylene groups adjacent to the *p*-phenylene unit ( $J_{\text{pr}}$  and  $J_{\text{st}}$ ), while the remaining two show more negative values:  $J_{\text{ng}} = -13.7$  and  $J_{\text{mo}} = -14.5$  Hz. The conformational dependence of geminal H,H couplings in methylene groups next to  $\pi$ -electron systems is known.<sup>29</sup> These couplings show the smallest absolute values when the nodal plane of the  $\pi$ -system and the vector joining the two methylene protons are oriented parallel to each other as is the case for [2.2]paracyclophane. The larger magnitude of  $J_{\text{ng}}$  and especially of  $J_{\text{mo}}$  seem to indicate that the molecule deviates from the idealized geometry by torsional deformation that moves one of the methylene C-H bonds at both  $\text{C}_X$  and  $\text{C}_U$  toward the planes formed by  $\text{C}_C$ ,  $\text{C}_F$ ,  $\text{C}_1$  and  $\text{C}_D$ ,  $\text{C}_E$ ,  $\text{C}_G$ , respectively. According to the larger magnitude of  $J_{\text{mo}}$ , this torsional deformation should be larger at  $\text{C}_U$ , which is reasonable with regard to the more severe steric repulsion expected between  $\text{H}_m$  and  $\text{H}_a$  than between  $\text{H}_n$  and  $\text{H}_d$ .

From the  $^{13}\text{C}$  satellites in the proton spectrum of **4**, the vicinal H,H couplings between the bridge protons are determined<sup>25</sup> to be 10.6 (cis) and 4.1 Hz (trans). In *ar*-mono- and *ar*-ortho-disubstituted derivatives one observes<sup>25</sup> little change in the cis couplings but a distinct decrease (down to 1 Hz) of one and a corresponding increase (up to 8 Hz) of the other trans coupling. Similar behavior is found for the  $\text{C}_W\text{-C}_X$  bridge in **7**. This suggests a twisting of the bridge in such a way that the torsional angle between the trans C-H bonds W-p and X-n decreases from  $120^\circ$  toward  $90^\circ$ . However, caution should be used in trying to apply Karplus-Conroy type relationships<sup>29</sup> to cases like these. The deformation of the bond angles from an ethane-like geometry may well make the Karplus-Conroy relationship inapplicable to paracyclophanes. The magnitudes of the vicinal couplings at the  $\text{C}_V\text{-C}_U$  bridge seem to support this cautionary note. Here both cis couplings are approximately 2 Hz smaller than in **4** whereas the trans couplings increase by 2.2 ( $J_{\text{ci}}$ ) and 0.6 Hz ( $J_{\text{ms}}$ ), respectively. In 1,2-disubstituted ethanes, however, any sizeable

(24) Fratini, A. private communication quoted in: Kechn, P. M., Rosenfeld, S. M. Eds. "Cyclophanes"; Academic Press: New York, 1983; Vol. 1, Chapter 3, pp 69-238.

(25) Ernst, L., unpublished observation.

(26) Haigh, C. W.; Mallion, R. B.; Armour, E. A. G. *Mol. Phys.* **1970**, *18*, 751-766.

(27) Berger, S.; Zeller, K. P. *Org. Magn. Reson.* **1978**, *11*, 303-307.

(28) Stothers, J. B.; Tan, C. T.; Wilson, N. K. *Org. Magn. Reson.* **1977**, *9*, 408-413.

(29) See, e.g.: Günther, H. "NMR Spectroscopy"; Wiley: Chichester, U.K., 1980. (a) pp 101-103. (b) pp 106-107.

increase of one trans coupling, caused by enlargement of the torsional angle from  $120^\circ$  to  $120^\circ + \alpha$ , should be accompanied by a similar decrease of the other trans coupling since the appropriate torsional angle decreases to  $120^\circ - \alpha$ . Evidently, details of the molecular geometry of the phenanthrenoparacyclophane will have to be determined by X-ray diffraction.

### Experimental Section

**General Methods:** Melting points were determined on a Kofler hot-stage apparatus and are uncorrected. IR spectra were taken on a Perkin-Elmer 157 G spectrometer and UV spectra on a Beckman UV 530 instrument. Low-resolution mass spectra were recorded on a MAT CH 7 instrument at 70 eV. For details of the NMR measurements see below.

**Synthesis. Preparation of trans-4-Styryl[2.2]paracyclophane (6).** A suspension of 0.32 g of sodium hydride in paraffin (60%) is placed in a 25-mL two-necked flask equipped with a magnetic stirrer and reflux condenser, and the paraffin is removed by careful washing with pentane. The apparatus is flame-dried, and 2.5 mL of absolute THF is added to the sodium hydride residue under stirring, followed by a solution of 1.79 g (7.83 mmol) of diethyl benzylphosphonate in 3 mL of THF. To complete the ylide formation the reaction mixture is warmed to  $40^\circ\text{C}$  for 30 min. After cooling to  $0^\circ\text{C}$  a solution of 1.55 g (6.55 mmol) of 4-formyl[2.2]paracyclophane (5)<sup>11</sup> in 10 mL of THF is added, and the olefination is completed by refluxing for 30 min. Hydrolysis, extraction with methylene chloride, and chromatography on neutral alumina (activity III-IV;  $\text{CCl}_4$ ) provide 1.2 g (59%) of 6: colorless needles (methylene chloride/methanol); mp  $153\text{--}154^\circ\text{C}$ ; IR (KBr)  $\nu_{\text{max}}$  2920 (m), 1590 (m), 1490 (m), 957 (s), 745 (m), 717 (m),  $682\text{ cm}^{-1}$  (m);  $^1\text{H}$  NMR ( $\text{CDCl}_3$ )  $\delta$  2.80-3.26 (7 H, m,  $\text{CH}_2\text{CH}_2$ ), 3.61 (1 H, m, bridge proton facing the 4-substituent), 6.36-6.77 (7 H, several m, aromatic H of paracyclophane part), 6.72 and 7.23 (2 H,  $J_{\text{AB}} = 16.0\text{ Hz}$ ,  $\text{CH}=\text{CH}$ ), 7.27-7.68 (5 H, several m, aromatic H of phenyl substituent); mass spectrum  $m/z$  (relative intensity) 310 ( $\text{M}^+$ , 31), 222 (21), 205 (100), 191 (68), 104 (45); UV (ethanol)  $\lambda_{\text{max}}$  318 ( $\epsilon = 19000$ ), 250 (sh, 11900), 226 nm (20800). Anal. Calcd for  $\text{C}_{24}\text{H}_{22}$ : C, 92.85; H, 7.14. Found: C, 92.57; H, 7.34.

**Preparation of [2.2](1,4)Phenanthrenoparacyclophane (7).** A solution of 155 mg (0.5 mmol) of 6 in 400 mL of cyclohexane is placed in an open beaker, a few crystals of iodine are added, and the vigorously stirred reaction mixture is irradiated for 3 h at room temperature with a high-pressure mercury lamp (Hanau, TQ 150). Brown deposits are removed from the solution by filtration, the solvent is evaporated, and the resulting crystalline residue is purified by thick-layer chromatography on silica (2:1  $\text{CCl}_4/\text{CHCl}_3$ ): 48 mg (31%) of [2.2](1,4)phenanthrenoparacyclophane (7), colorless plates (ethanol); mp  $169^\circ\text{C}$ ; IR (KBr)  $\nu_{\text{max}}$  2915 (ms), 2845 (m), 1495 (m), 1439 (m), 810 (s), 797 (m),  $715\text{ cm}^{-1}$  (s);  $^1\text{H}$  and  $^{13}\text{C}$  NMR spectra, see main section and below; mass spectrum  $m/z$  (relative intensity) 308 ( $\text{M}^+$ , 43), 203 (100), 189 (64), 104 (37), 84 (91); UV (ethanol)  $\lambda_{\text{max}}$  360 ( $\epsilon = 300$ ), 314 (5800), 279 (24500), 252 (20700), 215 nm (29000).

Anal. Calcd for  $\text{C}_{24}\text{H}_{20}$ : C, 93.46; H, 6.54. Found: C, 93.60; H, 7.11.

**NMR Spectra. General Methods.** NMR spectra were obtained on a Bruker AM 300 spectrometer ( $^1\text{H}$ , 300.1 MHz;  $^{13}\text{C}$ , 75.5 MHz) interfaced to an Aspect 3000 computer. Standard Bruker DISNMRP software (version 831101.1) was used. The sample was run at a concentration of 40 mg/0.55 mL of  $\text{CDCl}_3$  in a 5-mm-o.d. sample tube with a switchable  $^1\text{H}/^{13}\text{C}$  dual probe head. Chemical shift references were tetramethylsilane for  $^1\text{H}$  spectra (or residual  $\text{CHCl}_3$ ,  $\delta$  7.205) and  $\text{CDCl}_3$  for  $^{13}\text{C}$  spectra ( $\delta$  77.05). The durations of the  $90^\circ$  pulses were  $9.3\ \mu\text{s}$  ( $^1\text{H}$ , observe),  $14.3\ \mu\text{s}$  ( $^1\text{H}$ , decoupler at maximum power, ca. 10 W), and  $7.5\ \mu\text{s}$  ( $^{13}\text{C}$ , observe).

**Acquisition and Processing Parameters.** One-dimensional experiments:

(a) standard  $^1\text{H}$  spectra: spectral width (SW) 2100 Hz, 16K data points with zero filling to 32 K, Gaussian multiplication (LB =  $-1.3\text{ Hz}$ ,

GB = 0.3), digital resolution after Fourier transformation 0.13 Hz/point.

(b) homonuclear decoupling experiments: irradiation power level 15 dB below a nominal 0.2 W.

(c) NOE difference spectra (separate free induction decays were accumulated for the on-resonance irradiations and the control spectrum): prescan saturation time 10 s, decoupler power level 50 dB below 0.2 W, 360 scans and 4 dummy scans (DS) per irradiation frequency, exponential line broadening (LB) 0.3 Hz.

(d) standard  $^{13}\text{C}$  spectra: SW 18500 Hz, 32K data points, digital resolution 1.1 Hz/point, broad-band and single-frequency off-resonance decoupling.

(e) proton-coupled  $^{13}\text{C}$  spectrum: SW 1370 Hz (aromatic region only), 4K data points with zero filling to 8K, Gaussian multiplication (LB =  $-1.0\text{ Hz}$ , GB = 0.28), digital resolution 0.33 Hz/point,  $90^\circ$  pulses, no. of scans (NS) = 4500, 1.5-s prescan decoupling period.

Two-dimensional experiments:

(a) Standard homonuclear  $^1\text{H}/^1\text{H}$  correlation (COSY-45): pulse sequence<sup>13b</sup>  $D_1-90^\circ-t_1-45^\circ-t_2$  (=acquisition) with  $D_1 = 0.5\text{ s}$  and  $t_1$  incremented from  $3\ \mu\text{s}$  to 142 ms in 256 steps of  $556\ \mu\text{s}$ , SW2 1800 Hz (quadrature detection), data table (TD) of 512 words, SW1  $\pm 900\text{ Hz}$  (quadrature detection by phase cycling)<sup>15c</sup>, NS = 16 and DS = 4 acquired for each value of  $t_1$ , total time 1 h. The resulting data matrix was zero-filled once in each dimension ( $F_1$  and  $F_2$ ) and multiplied by a sine-bell function yielding, after double Fourier transformation, a 256K matrix of real points. The digital resolution was 3.5 Hz/point in both  $F_1$  and  $F_2$ . After symmetrization the data were displayed as a contour level plot in the magnitude mode.

(b)  $^1\text{H}/^1\text{H}$  correlation with emphasis of long-range couplings (COSY-45 LR): pulse sequence<sup>13b</sup>  $D_1-90^\circ-D_2-t_1-45^\circ-D_2-t_2$ ,  $D_1 = 0.5\text{ s}$ ,  $D_2$  (optimized for  $J_{\text{HH}} = 0.6\text{ Hz}$ ) = 417 ms,  $t_1$  incremented from  $3\ \mu\text{s}$  to 280 ms in 512 steps of  $546\ \mu\text{s}$ , SW1  $\pm 916\text{ Hz}$ , SW2 1832 Hz, TD = 1K, NS = 16, DS = 2, total time 4.5 h. Data treatment as in (a) gave a 1024K real point matrix, digital resolution 1.8 Hz/point in  $F_1$  and  $F_2$ .

(c) Heteronuclear  $^{13}\text{C}/^1\text{H}$  correlation with polarization transfer via  $^1J_{\text{CH}}$  and suppression of vicinal and longer range  $^1\text{H},^1\text{H}$  couplings: pulse sequence<sup>19</sup>  $D_1-90^\circ_x(^1\text{H})-t_1/2-90^\circ_y(^1\text{H})-D_3-180^\circ_x(^1\text{H}), 180^\circ_x(^{13}\text{C})-D_3-90^\circ_y(^1\text{H})-t_1/2-D_3-90^\circ_x(^1\text{H}), 90^\circ_x(^{13}\text{C})-D_4-t_2$  (=acquisition with broad-band  $^1\text{H}$  decoupling),  $D_1 = 0.5\text{ s}$ ,  $D_3 = (2J_{\text{CH}})^{-1} = 3.45\text{ ms}$ ,  $D_4 = (3.5J_{\text{CH}})^{-1} = 1.97\text{ ms}$ , assuming an average  $^1J_{\text{CH}}$  of 145 Hz,  $t_1/2$  incremented from  $3\ \mu\text{s}$  to 67 ms in 256 steps of  $260\ \mu\text{s}$ , SW1 ( $^1\text{H}$ )  $\pm 962\text{ Hz}$  ( $\delta_{\text{H}}$  8.82-2.41), SW2 ( $^{13}\text{C}$ ) 8197 Hz ( $\delta_{\text{C}}$  140.2-31.6), TD = 1K, NS = 288, DS = 4, total time 13.5 h, data treatment as in (a) apart from symmetrization, 512K real point matrix, digital resolution 8.0 Hz/point in  $F_2$  ( $^{13}\text{C}$ ) and 3.8 Hz/point in  $F_1$  ( $^1\text{H}$ ).

(d)  $^{13}\text{C}/^1\text{H}$  correlation with polarization transfer via long-range  $J_{\text{CH}}$ : pulse sequence<sup>14,15c</sup>  $D_1-90^\circ(^1\text{H})-t_1/2-180^\circ(^1\text{H}), 180^\circ(^{13}\text{C})-t_1/2-D_3-90^\circ(^1\text{H}), 90^\circ(^{13}\text{C})-D_4-t_2$ ,  $D_1 = 0.5\text{ s}$ ,  $D_3 = 83.3\text{ ms}$ ,  $D_4 = 47.6\text{ ms}$ , i.e., optimization for  $^1J_{\text{CH}} = 6\text{ Hz}$ ,  $t_1/2$  incremented from  $3\ \mu\text{s}$  to 71 ms in 256 steps of  $278\ \mu\text{s}$ , SW1 ( $^1\text{H}$ )  $\pm 900\text{ Hz}$ , SW2 ( $^{13}\text{C}$ ) 1359 Hz (aromatic region only), TD = 1K, NS = 192, DS = 2, total time 15 h, data treatment as in (a) apart from symmetrization, power-mode display to increase signal/noise; 512K real point matrix, digital resolution 1.3 Hz/point in  $F_2$  ( $^{13}\text{C}$ ) and 3.5 Hz/point in  $F_1$  ( $^1\text{H}$ ).

The spin systems (a, b, e, f), (i, j, k, l), (m, o, s, t), and (n, p, q, r) in the one-dimensional proton spectrum were analyzed separately with a locally modified version of the LAOCN3 program.<sup>30</sup> After iteration, root-mean-square errors between observed and calculated transitions were between 0.025 and 0.048 Hz. Experimental frequencies were assigned to 78-100% of the transitions, depending on the degree of overlap and the number of lines of sufficient intensity.

**Registry No. 5,** 729-30-6; **6,** 98395-17-6; **7,** 98395-18-7; diethyl benzylphosphonate, 1080-32-6.